materials

MDPI

Article

Reduction of Thermal Conductivity for Icosahedral Al-Cu-Fe Quasicrystal through Heavy Element Substitution

Yoshiki Takagiwa [1,*], Ryota Maeda [1], Satoshi Ohhashi [2] and An-Pang Tsai [2]

[1] National Institute for Materials Science (NIMS), 1-2-1 Sengen, Tsukuba 305-0047, Ibaraki, Japan; ryota-maeda@denka.co.jp
[2] Institute of Multidisciplinary Research for Advanced Materials (IMRAM), Tohoku University, 2-1-1 Katahira, Sendai 980-8577, Japan; satoshi.ohhashi.d4@tohoku.ac.jp (S.O.); aptsai@tagen.tohoku.co.jp (A.-P.T.)
* Correspondence: TAKAGIWA.Yoshiki@nims.go.jp

Abstract: Icosahedral Al-Cu-Fe quasicrystal (QC) shows moderate electrical conductivity and low thermal conductivity, and both p- and n-type conduction can be controlled by tuning the sample composition, making it potentially suited for thermoelectric materials. In this work, we investigated the effect of introducing chemical disorder through heavy element substitution on the thermal conductivity of Al-Cu-Fe QC. We substituted Au and Pt elements for Cu up to 3 at% in a composition of $Al_{63}Cu_{25}Fe_{12}$, i.e., $Al_{63}Cu_{25-x}(Au,Pt)_xFe_{12}$ (x = 0, 1, 2, 3). The substitutions of Au and Pt for Cu reduced the phonon thermal conductivity at 300 K ($\kappa_{ph,300K}$) by up to 17%. The reduction of $\kappa_{ph,300K}$ is attributed to a decrease in the specific heat and phonon relaxation time through heavy element substitution. We found that increasing the Pt content reduced the specific heat at high temperatures, which may be caused by the locked state of phasons. The observed glass-like low values of $\kappa_{ph,300K}$ (0.9–1.1 W m^{-1} K^{-1} at 300 K) for $Al_{63}Cu_{25-x}(Au,Pt)_xFe_{12}$ are close to the lower limit calculated using the Cahill model.

Keywords: quasicrystals; thermal conductivity; Al-Cu-Fe; heavy element substitution; thermoelectric properties

check for updates

Citation: Takagiwa, Y.; Maeda, R.; Ohhashi, S.; Tsai, A.-P. Reduction of Thermal Conductivity for Icosahedral Al-Cu-Fe Quasicrystal through Heavy Element Substitution. *Materials* **2021**, *14*, 5238. https://doi.org/10.3390/ma14185238

Academic Editors: Li-Dong Zhao and Lidong Chen

Received: 27 August 2021
Accepted: 10 September 2021
Published: 12 September 2021

Publisher's Note: MDPI stays neutral with regard to jurisdictional claims in published maps and institutional affiliations.

Copyright: © 2021 by the authors. Licensee MDPI, Basel, Switzerland. This article is an open access article distributed under the terms and conditions of the Creative Commons Attribution (CC BY) license (https://creativecommons.org/licenses/by/4.0/).

1. Introduction

Thermoelectric materials can directly convert a temperature difference into electrical voltage. Home heating, automotive exhaust, and industrial processes all generate enormous waste heat. Thermoelectric materials can recover waste heat emitted from commercial and industrial cycles. The potential of thermoelectric materials can be evaluated by the dimensionless figure of merit zT, as expressed by

$$zT = \frac{S^2\sigma}{\kappa_t}T, \quad (1)$$

where S, σ, κ_t, and T are the Seebeck coefficient, the electrical conductivity, the total thermal conductivity, and the temperature, respectively [1,2]. In general, κ_t is the sum of two contributions, the phonon part κ_{ph} and the electron part κ_{el}.

$$\kappa_t = \kappa_{ph} + \kappa_{el} \quad (2)$$

To enhance zT, it is necessary to simultaneously optimize S, σ, and κ_t. Icosahedral quasicrystals (QCs) have shown good thermoelectric properties because of the formation of the pseudogap and complex crystal structures [3]. We succeeded in an enhancement of zT for $Al_{71}Pd_{20}Mn_9$ QC from 0.18 to 0.26 through 3 at% Ga substitution for Al without reducing the power factor $S^2\sigma$. Substitution of Ga at less than 4 at% for Al had less influence on both σ and S, while κ_t (in particular, κ_{ph}) decreased through the combination of weakening of the intercluster bonds and an alloying effect [3–5].

Icosahedral Al-Cu-Fe QC shows the following attractive characteristics as a potential thermoelectric material:

(i) The magnitude and sign of the Seebeck coefficient strongly depend on the sample composition, i.e., the position of the Fermi level in the electronic density of states, indicating that both p- and n-type materials can be obtained in the same alloy [6–8].
(ii) As expected from a complex crystal structure, a low κ_t of less than 2 W m^{-1} K^{-1} at 300 K has been reported [7–10].
(iii) The constituent elements are nontoxic, readily available, and show favorable costs for industrial use [11].

Although several advantageous physical properties are recognized in Al-Cu-Fe QC, there are only a few studies on the high-temperature thermoelectric properties [9,12]. Until now, the effect of elemental substitution on the thermoelectric properties of Al-Cu-Fe QC has not been clarified. In particular, lowering κ_{ph} using an alloying effect, inspired from previous works [4,13,14] on Al-Pd-Mn and Al-Pd-Re QCs by transition metal substitutions, remains a possibility. We also expected that the suppression of phason flipping by heavy element substitution could reduce the thermal conductivity. In this work, we focus on icosahedral Al-Cu-Fe QC for lowering κ_t and investigate the effects of Au and Pt substitutions for Cu on κ_{ph}. Here, we selected Au and Pt as substitution elements for Cu because of the large atomic radii, strong bond strength with Al, and a high melting point of Pt. From the experimental point of view, investigating high-temperature thermal conductivity is of great importance for controlling the unusual increase in the specific heat [15–19] for Al-based QCs and approximants, which provides an additional route to tune the thermoelectric [3] and thermal rectifier [12] properties.

2. Experimental Procedure and Sample Characterization

Mother ingots of $Al_{63}Cu_{25-x}(Au,Pt)_xFe_{12}$ (x = 0, 1, 2, 3) were synthesized by an arc melting technique and annealed at 1073 K for 48 h under a purified argon atmosphere. The obtained ingots were crushed to a particle size of less than 45 μm. The regulated powder samples were put into a carbon die with an inner diameter of 10 mm for spark plasma sintering with a heating rate of ~150 K min^{-1} (LABOX-110MC; SinterLand, Inc., Niigata, Japan). A pressure of 57 MPa was applied under a purified argon atmosphere during the sintering process. The consolidating temperature was maintained for 10 min for all samples. Table 1 lists applied consolidating temperatures, bulk densities obtained from geometric calculations, and crystalline sizes using Scherrer's formula for $Al_{63}Cu_{25-x}(Au,Pt)_xFe_{12}$ (x = 0, 1, 2, 3). The resulting relative densities were over 95%. The bulk density increased with increasing Au and Pt fraction x, which can be understood as increasing the average mass through heavy element substitution. The estimated crystalline sizes were slightly larger than the value (850 Å) of the NIST Si standard powder sample. The phase purity of the samples was evaluated by X-ray diffraction (XRD) (SmartLab; Rigaku, Inc., Tokyo, Japan), as shown in Figure 1a,b. We observed peak shifting to a lower degree with increasing (Au,Pt) concentrations, indicating that the quasilattice constant increased (Figure 2). This behavior can be qualitatively explained by the substitution of larger atomic radii of Au (1.37Å) and Pt (1.39Å) for Cu (1.28Å). Only the sample of $Al_{63}Cu_{22}Au_3Fe_{12}$ contained a small amount of the excess phase of Al_2Au. The precipitates can affect the thermoelectric properties; thus, we excluded the results and discussion for $Al_{63}Cu_{22}Au_3Fe_{12}$. Composition analyses were performed using inductively coupled plasma atomic emission spectroscopy (ICP) analysis (Table 2). We found that the analyzed Au/Pt concentration increased with increasing nominal fraction, except for the sample of $Al_{63}Cu_{22}Au_3Fe_{12}$, in which the secondary phase of Al_2Au was precipitated. From ICP analysis, we found that Au hardly substitutes for Cu, while Pt can substitute for Cu up to 3 at%.

Table 1. List of applied consolidating temperatures, bulk densities, crystalline sizes for $Al_{63}Cu_{25-x}(Au,Pt)_xFe_{12}$ (x = 0, 1, 2, 3).

Samples	Consodidating Temperature (K)	Bulk Density (g cm^{-3})	Crystalline Size (Å)
$Al_{63}Cu_{25}Fe_{12}$	898	4.43	1256(62)
$Al_{63}Cu_{24}Au_1Fe_{12}$	1013	4.58	1090(58)
$Al_{63}Cu_{23}Au_2Fe_{12}$	1018	4.70	824(70)
$Al_{63}Cu_{22}Au_3Fe_{12}$	1033	4.80	379(13)
$Al_{63}Cu_{24}Pt_1Fe_{12}$	948	4.66	1062(16)
$Al_{63}Cu_{23}Pt_2Fe_{12}$	968	4.86	979(17)
$Al_{63}Cu_{22}Pt_3Fe_{12}$	1083	4.88	974(16)

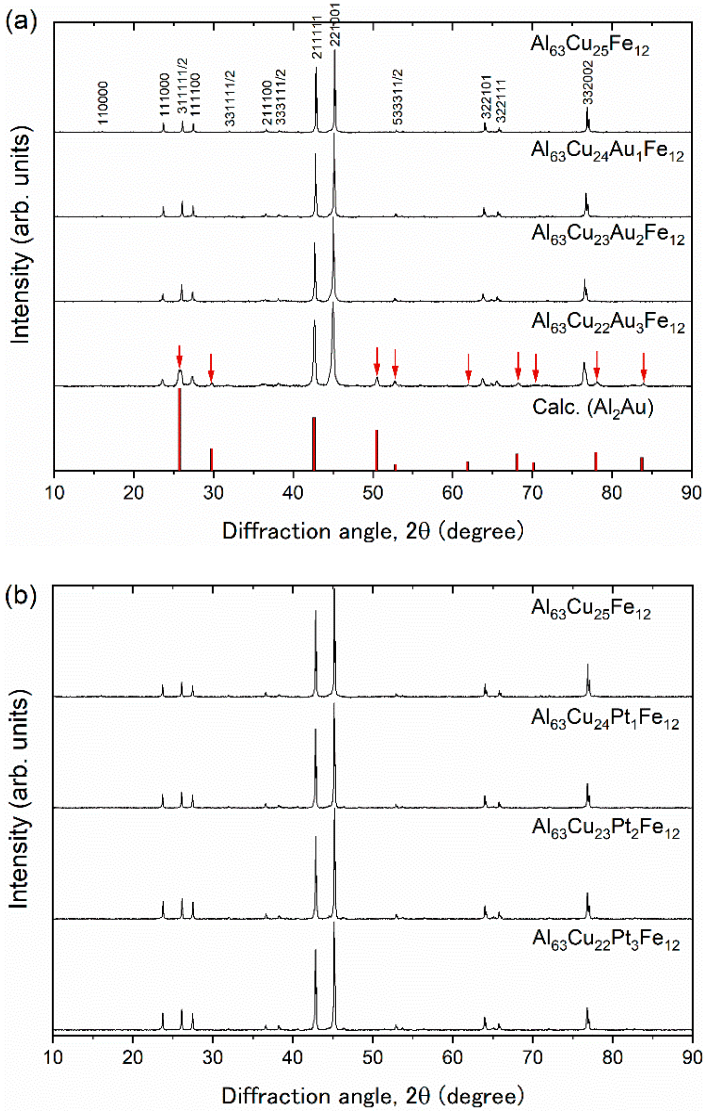


Figure 1. X-ray diffraction patterns of (**a**) $Al_{63}Cu_{25-x}(Au,Pt)_xFe_{12}$ (x = 0, 1, 2, 3), together with peak indices and calculated peak positions of Al_2Au, and (**b**) $Al_{63}Cu_{25-x}Pt_xFe_{12}$ (x = 0, 1, 2, 3). Arrows indicate peaks of excess phase of Al_2Au.

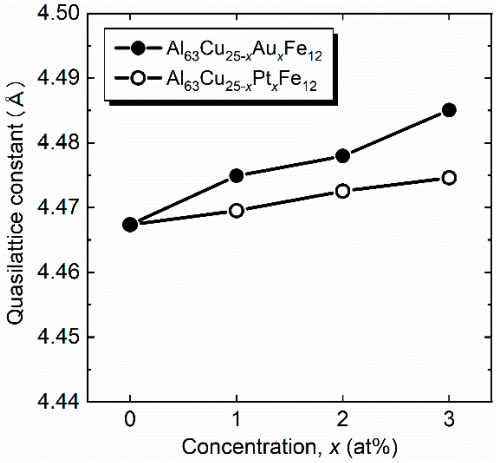


Figure 2. Quasilattice constant of $Al_{63}Cu_{25-x}(Au,Pt)_xFe_{12}$ (x = 0, 1, 2, 3).

Table 2. Nominal compositions and ICP results for $Al_{63}Cu_{25-x}(Au,Pt)_xFe_{12}$ (x = 1, 2, 3).

Nominal Compositions	Phase	ICP Analysis of Chemical Composition
$Al_{63}Cu_{24}Au_1Fe_{12}$	*i*	$Al_{63.1}Cu_{24.2}Au_{0.9}Fe_{11.8}$
$Al_{63}Cu_{24}Au_2Fe_{12}$	*i*	$Al_{64}Cu_{22.4}Au_{1.9}Fe_{11.7}$
$Al_{63}Cu_{22}Au_3Fe_{12}$	*i* + Al_2Au	$Al_{65.7}Cu_{21.2}Au_{1.7}Fe_{11.4}$
$Al_{63}Cu_{24}Pt_1Fe_{12}$	*i*	$Al_{63.2}Cu_{24.2}Pt_{0.9}Fe_{11.3}$
$Al_{63}Cu_{24}Pt_2Fe_{12}$	*i*	$Al_{63.2}Cu_{23.8}Pt_{1.7}Fe_{11.3}$
$Al_{63}Cu_{22}Pt_3Fe_{12}$	*i*	$Al_{63.1}Cu_{22.3}Pt_{2.6}Fe_{12}$

The total thermal conductivity κ_t was calculated from the density d, the specific heat at constant pressure C_P, and the thermal diffusivity λ using the relationship $\kappa_t = d \cdot C_P \cdot \lambda$. Both C_P and λ were measured by the laser flash method (TC-7000; Advance Riko, Inc., Kanagawa, Japan) from 300 to 873 K. The transverse and longitudinal speeds of sound were measured by ultrasonic pulse-echo method (Echometer 1062; Nihon Matech Corp., Tokyo, Japan). The electrical conductivity was measured between 300 K and 873 K by the four-probe method (ZEM-3; Advance Riko, Inc., Kanagawa, Japan) for a rough estimation of the electron thermal conductivity κ_{el} using the Wiedemann–Franz law. The Seebeck coefficient was obtained by the steady-state temperature gradient method using a ZEM-3 instrument.

3. Results and Discussion

Figure 3a,b show the temperature dependences of C_P and λ from 300 to 873 K for $Al_{63}Cu_{25-x}(Au,Pt)_xFe_{12}$ (x = 0, 1, 2, 3). The measured C_P of $Al_{63}Cu_{25}Fe_{12}$ increased with increasing temperature and reached between 4R and 5R at 873 K, as shown in Figure 3a. This behavior is quantitatively consistent with a previous report by Prekul et al. [16]. An unusual increase in the C_P of icosahedral and decagonal QCs was discussed in terms of the introduction of chemical disorder and anharmonicity in lattice vibration [15] and the localized electronic nature [16] of QCs. Edagawa et al. first mentioned that excess specific heat can be attributed to the excitation of phasons [15], which will be discussed below. The values of C_P at 300 K for both Au- and Pt-substituted samples decreased with increasing x because of an increase in mean atomic weight. However, the trend of C_P at high temperatures is rather complex; the C_P values of Au- and Pt-substituted samples, except for a sample with x = 3 (Pt), were larger than that of pristine Al-Cu-Fe. Here, we exclude the detailed discussion on C_P of Au-substituted samples because Au did not systematically substitute for Cu, as already mentioned in Section 2. It is easily expected that increasing Pt fraction will bring chemical disorder in the atomic arrangement. Therefore, the observed increase in C_P at high temperatures for samples with x = 1 and 2 can be caused by introducing chemical disorder. On the contrary, the systematic decrease in C_P at 873 K

with increasing Pt fraction was observed; in particular, the C_P of the sample with $x = 3$ was lower than that of $Al_{63}Cu_{25}Fe_{12}$ QC. The observed reduction of C_P at high temperatures may be attributed to the locked state of phasons, that is, a pinning effect of phasons through heavy element substitution for Cu sites. However, there is room for further discussion on the effect of excited or locked phasons on the high-temperature specific heat, which will enhance our knowledge of the specific features of QCs. On the other hand, as expected, the λ values were reduced by both Au and Pt substitutions throughout the measurement temperature region because of the alloying effect, as shown in Figure 3b.

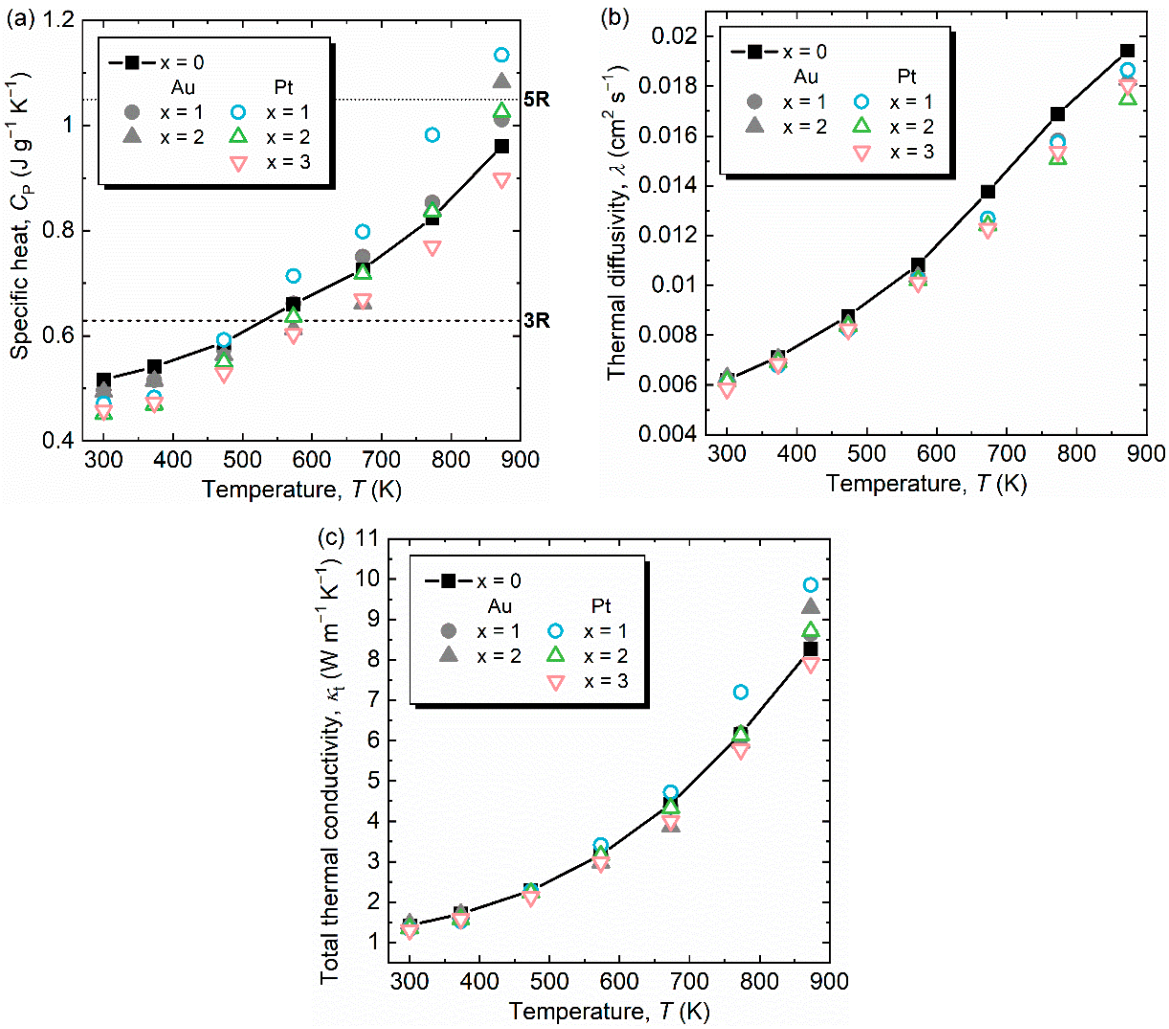


Figure 3. (**a**) Specific heat at constant pressure C_P, (**b**) thermal diffusivity λ, and (**c**) total thermal conductivity κ_t as a function of temperature for $Al_{63}Cu_{25-x}(Au,Pt)_xFe_{12}$ ($x = 0, 1, 2, 3$). The dashed and dotted lines represent the Dulong–Petit limit ($3R$) and $5R$, respectively. $Al_{63}Cu_{22}Au_3Fe_{12}$ is excluded because of secondary phase precipitation.

The temperature dependence of obtained κ_t for all samples is displayed in Figure 3c. The value of κ_t at 300 K ($\kappa_{t,300K}$) for $Al_{63}Cu_{25}Fe_{12}$ is 1.42 W m^{-1} K^{-1}; previously reported $\kappa_{t,300K}$ of Al-Cu-Fe QC is distributed in the range of 1−2 W m^{-1} K^{-1} [7–10], which is caused by the difference in the sample composition because κ_t (in particular, κ_{el}) is sensitive to the actual composition, as observed in Al-Pd-Re QC [20]. However, the details are not clear at this stage because the analyzed composition and each parameter of d, C_P, and λ were not described in the literature [7–10]. Compared with other Al-based QCs, the measured $\kappa_{t,300K}$ of $Al_{63}Cu_{25}Fe_{12}$ is significantly higher than those of Al-Pd-Mn and Al-Pd-Re QCs [3,20] because of the relatively light constituent elements Fe and Co, compared with Pd and Re. A detailed comparison will be discussed below.

Table 3 lists the $\kappa_{t,300K}$ for all samples investigated. While the $\kappa_{t,300K}$ for Au-substituted samples increased by up to 2.8%, the $\kappa_{t,300K}$ for Pt-substituted samples decreased by up to 7.7%. To understand the different behaviors of $\kappa_{t,300K}$ with Au and Pt substitutions, we evaluated the lattice component of κ_{ph} after subtracting κ_{el} from κ_t using the Wiedemann–Franz law:

$$\kappa_{ph} = \kappa_t - \kappa_{el} = \kappa_t - L_0 \sigma T \quad (3)$$

where L_0 is the Lorenz number. We estimated L_0 value using a model proposed by Kim et al., L_0 = 1.5 + exp[$-|S|/116$]*10^{-8} V^2 K^{-2} [21]. The electrical conductivity σ and calculated κ_{el} as a function of temperature are displayed in Figure 4a,b. All samples show semiconductor-like behavior, i.e., σ increases with increasing temperature [Figure 4a]; thus, the estimated κ_{el} also increases monotonically [Figure 4b]. The measured σ at 300 K (σ_{300K}) for $Al_{63}Cu_{25}Fe_{12}$ was approximately 400 Ω^{-1} cm^{-1}, which is consistent with previous data of similar sample compositions of Al-Cu-Fe QC [6–8,10]. Contrary to expectation, σ significantly increased with Au substitution (σ_{300K} ~700 Ω^{-1} cm^{-1}), although Cu and Au have the same number of electrons per atom ratio (e/a) of +1 [22]. Referring to the results of ICP composition analyses (Table 2), the Al concentration of Au-substituted samples increased as x increases. Therefore, the measured enhancement of σ will be caused by the different Al/(Cu+Au) ratios, i.e., shifting the position of the Fermi level in the electronic density of states. On the other hand, Pt substitution for Cu succeeds in more precise composition control with almost constant Al concentration. The sample with x = 1 (Pt) possessed a higher σ_{300K} of 550 Ω^{-1} cm^{-1}, probably because of an increase in the carrier concentration, compared with the sample with x = 0. In turn, the carrier mobility of samples with higher Pt fractions of x = 2, 3 will be largely suppressed by introducing chemical disorder, resulting in a decrease in σ for the samples with x = 2 and 3. Although the microstructure (such as defect, strain, and grain size) can also affect σ, the observed non-monotonic change in σ cannot be explained only by such extrinsic factors.

Table 3. Total thermal conductivity at 300 K ($\kappa_{t,300K}$) and its rate of change ($\Delta\kappa_{t,300K}/\kappa_{t,300K}$), phonon thermal conductivity at 300 K ($\kappa_{ph,300K}$) and its rate of change ($\Delta\kappa_{ph,300K}/\kappa_{ph,300K}$), rate of change in specific heat at 300 K ($\Delta C_{P,300K}/C_{P,300K}$), rate of change in speed of sound ($\Delta v_s/v_s$), and minimum thermal conductivity at 300 K ($\kappa_{min,300K}$) for $Al_{63}Cu_{25-x}(Au,Pt)_xFe_{12}$ (x = 0, 1, 2, 3). $Al_{63}Cu_{22}Au_3Fe_{12}$ is excluded because of secondary phase precipitation.

Samples	$\kappa_{t,300K}$	$\Delta\kappa_{t,300K}/\kappa_{t,300K}$	$\kappa_{ph,300K}$	$\Delta\kappa_{ph,300K}/\kappa_{ph,300K}$
	(W m^{-1} K^{-1})	(%)	(W m^{-1} K^{-1})	(%)
x = 0	1.42	-	1.12	-
Au: x = 1	1.41	−0.7	0.96	−14.3
Au: x = 2	1.46	2.8	1.06	−5.4
Pt: x = 1	1.33	−6.3	0.93	−17.0
Pt: x = 2	1.35	−4.9	1.03	−8.0
Pt: x = 3	1.31	−7.7	1.03	−8.0
Samples	$\Delta C_{P,300K}/C_{P,300K}$	$\Delta v_s/v_s$	$\kappa_{min,300K}$	
	(%)	(%)	(W m^{-1} K^{-1})	
x = 0	-	-	1.11	
Au: x = 1	−3.9	−0.2	1.11	
Au: x = 2	−4.5	−5.2	1.08	
Pt: x = 1	−8.7	−0.2	1.13	
Pt: x = 2	−13	−2.3	1.12	
Pt: x = 3	−11	0	1.14	

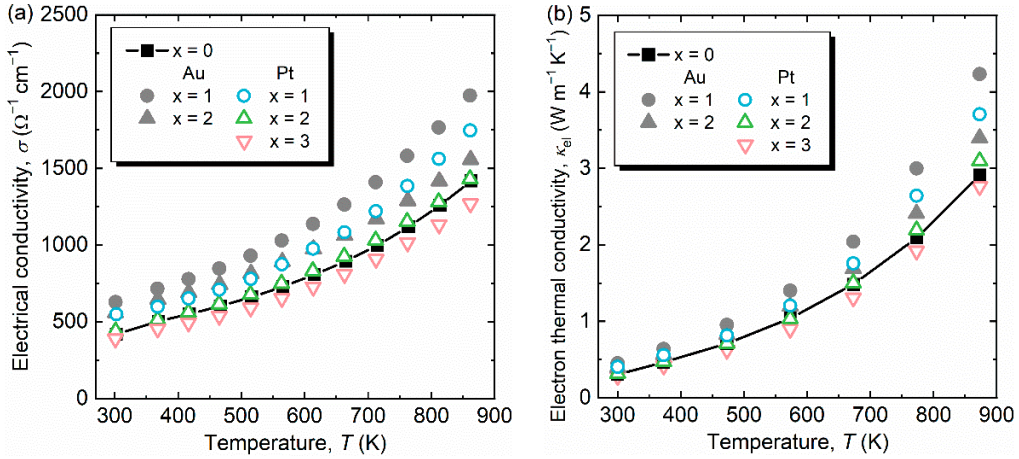


Figure 4. (**a**) Electrical conductivity σ and (**b**) electron thermal conductivity κ_{el} as a function of temperature for $Al_{63}Cu_{25-x}(Au,Pt)_xFe_{12}$ (x = 0, 1, 2, 3). $Al_{63}Cu_{22}Au_3Fe_{12}$ is excluded because of secondary phase precipitation.

Returning to the estimation of κ_{el}, the Wiedemann–Franz law applied for pseudogap and narrow-gap compounds is found to be invalid because it assumes that the spectral conductivity varies linearly with energy [17]. The validity of the Wiedemann–Franz law was also discussed by Maciá [23]. Hitherto, there is no empirical relation to calculate κ_{el} for QCs; thus, we adopted the conventional Equation (3) and L_0 values using an empirical model [21] for a rough estimation of κ_{ph}.

The calculated κ_{ph} as a function of temperature are shown in Figure 5a,b. It should be noted that although the apparent increase in κ_{ph} at high temperatures originates from conduction carriers [17], room-temperature κ_{ph} may not be largely under- or over-estimated. We found that the increase in $\kappa_{t,300K}$ for Au-substituted samples (Table 3) is attributed to an increase in κ_{el}, as shown in Figure 4b, probably because of an increase in the carrier concentration because the electrical conductivity increases for Au-substituted Al-Cu-Fe [Figure 4a]. The κ_{ph} at 300 K ($\kappa_{ph,300K}$) for both Au- and Pt-substituted samples decreased by up to 14.3% and 17.0%, respectively (Table 3), which is caused by the alloying effect. For a better understanding of the decrease in $\kappa_{ph,300K}$, we performed speed-of-sound measurements for pristine and Au- and Pt-substituted samples. The obtained speeds of sound v_s are distributed between 4150–4400 m s^{-1}, and no composition dependence of v_s is observed. Here, κ_{ph} is expressed using the specific heat at constant volume C_V, v_s, and the phonon relaxation time τ_{ph},

$$\kappa_{ph} = \frac{1}{3} C_V v_s^2 \tau_{ph} \quad (4)$$

We now compare each parameter change of C_P and v_s, as listed in Table 3. Here, we should discuss C_V rather than C_P using the following relationship [15]:

$$C_V = C_P - 9VB\alpha^2 T \quad (5)$$

where V, B, and α are the atomic volume, the bulk modulus, and the linear thermal expansion coefficient, respectively. Although we did not perform measurements of B and α, qualitative analysis can be performed using the parameter C_P. The rate of change in C_P, $\Delta C_{P,300K}/C_{P,300K}$, increased with increasing Au/Pt fraction; the reduction of C_P at 300 K for Pt-substituted samples is larger than that for Au-substituted samples. On the other hand, the rate of change in v_s, $\Delta v_s/v_s$ had less influence on $\kappa_{ph,300K}$. However, the additional reduction of τ_{ph} should be considered to explain $\Delta\kappa_{ph,300K}/\kappa_{ph,300K}$ of 14.3% and 17.0% for Au- and Pt-substituted samples, respectively. The reduction of τ_{ph} is estimated to be up to ~11%, and the alloying effect through heavy element substitution, in particular, worked in dilute Au- and Pt-substituted Al-Cu-Fe QC.

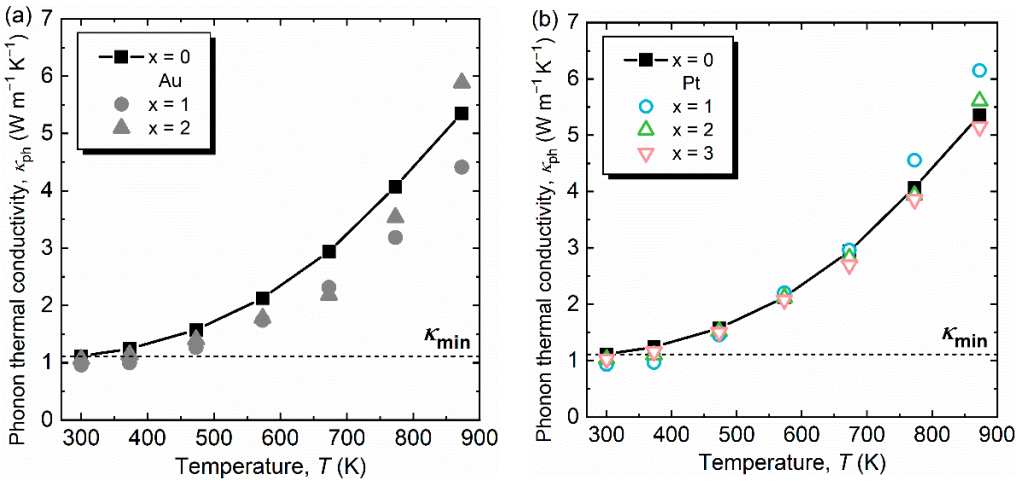


Figure 5. Phonon thermal conductivity κ_{ph} as a function of temperature for (**a**) $Al_{63}Cu_{25-x}Au_xFe_{12}$ (x = 0, 1, 2) and (**b**) $Al_{63}Cu_{25-x}Pt_xFe_{12}$ (x = 0, 1, 2, 3). The dashed lines represent the minimum thermal conductivity κ_{min} for $Al_{63}Cu_{25}Fe_{12}$.

Next, we evaluated the minimum thermal conductivity κ_{min} using the model proposed by Cahill et al. [24,25], which provides the lower limit of the lattice thermal conductivity for amorphous solids and disordered crystals. The κ_{min} can be calculated as the following equation,

$$\kappa_{min} = \left(\frac{\pi}{6}\right)^{\frac{1}{3}} k_B n^{\frac{2}{3}} \sum_{l,t} v_{l,t} \left(\frac{T}{\theta_{l,t}}\right)^2 \int_0^{\frac{\theta_{l,t}}{T}} \frac{x^3 e^x}{(e^x - 1)^2} dx \quad (6)$$

Here, k_B is the Boltzmann constant, n is the number density of atoms, v_l is the longitudinal speed of sound, v_t is the transverse speed of sound, T is the temperature, and $\theta_{l,t}$ is the cut off temperature, $\theta_{l,t} = v_{l,t}\left(\frac{\hbar}{k_B}\right)(6\pi^2 N)^{\frac{1}{3}}$, where $\hbar$ is Planck's constant. The calculated κ_{min} is listed in Table 3. Note here that the values of $\kappa_{ph,300K}$ for $Al_{63}Cu_{25-x}(Au,Pt)_xFe_{12}$ are already close to the κ_{min}, indicating that extra phonon engineering such as nanostructuring [26] will not be beneficial for further reduction of κ_{ph} of the present materials.

Finally, we compare $\kappa_{ph,300K}$ for various three-dimensional icosahedral QCs and related approximant crystals (AC): Al-Cu-Fe QC, Al-Cu-(Au,Pt)-Fe QCs, Al-Pd-Mn QC [3], Al-Pd-Re QC, and Tsai-type cubic-Au-Al-Gd AC [27], as shown in Figure 6. Compared with Al-based ternary QCs, Al-Cu-Fe QC having a lighter mean atomic weight shows the highest $\kappa_{ph,300K}$, while Al-Pd-Re QC shows the lowest one. A significant increase in d results in a low v_s, $v_s = \sqrt{B/d}$. Indeed, the values of v_s are 4340, 3770, and 3590 m s^{-1} for Al-Cu-Fe QC, Al-Pd-Mn QC [4], and Al-Pd-Re QC, respectively. Note here again that the decrease in $\kappa_{ph,300K}$ of Au- and Pt-substituted Al-Cu-Fe QCs is attributed to the reduction of both C_P and τ_{ph}. Recently discovered Tsai-type Au-based approximant ACs have rather heavy atomic weight, close to 130 g mol^{-1}. One example is cubic-Au-Al-RE ACs; a glass-like low $\kappa_{ph,300K}$ of ~0.6 W m^{-1} K^{-1} was observed for Au-Al-Gd AC. Cubic-Au-Al-RE ACs may be a good starting point for enhancing thermoelectric properties because they possess wide composition ranges [28]. Compared with pristine Al-Cu-Fe, the Au/Pt substitution brings a heavier atomic weight of up to 10%. The $\kappa_{ph,300K}$ of Au/Pt-substituted quaternary Al-Cu-Fe has a value close to that of ternary Al-Pd-Mn QC [3], in which a heavier mean atomic weight is expected.

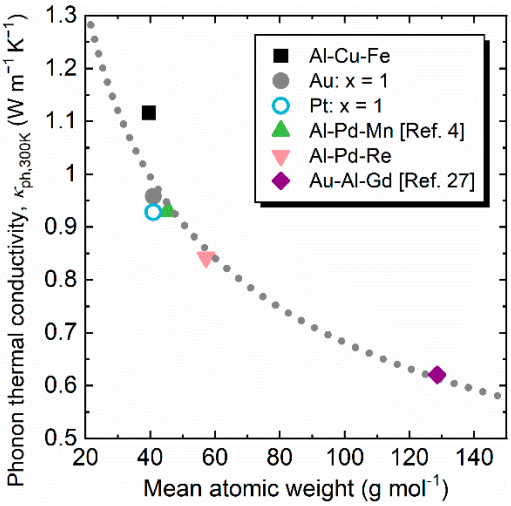


Figure 6. Phonon thermal conductivity at 300 K $\kappa_{ph,300K}$ versus mean atomic weight for various undoped icosahedral quasicrystals (QCs) and related approximant crystals (ACs): Al-Cu-Fe QC, Al-Cu-(Au,Pt)-Fe QCs, Al-Pd-Mn QC [4], Al-Pd-Re QC, and cubic-Au-Al-Gd AC [27]. The Au/Pt substitution reduced $\kappa_{ph,300K}$ down to that of Al-Pd-Mn QC [4]. The dashed curve is drawn to guide the eye.

4. Conclusions

We investigated the effects of Au and Pt substitutions on the thermal conductivity above 300 K for $Al_{63}Cu_{25-x}(Au,Pt)_xFe_{12}$ (x = 0, 1, 2, 3). High-density Au- and Pt-substituted Al-Cu-Fe samples were successfully synthesized by the combination of arc melting and spark plasma sintering. We found that increasing the Pt content reduced the specific heat at high temperatures, which may be caused by the locked state of phasons. The substitution of Pt for Cu reduced $\kappa_{ph,300K}$ by up to 17%. The reduction of $\kappa_{ph,300K}$ was attributed to a decrease in the specific heat and phonon relaxation time through heavy element substitution and the alloying effect. The present results show that the substitution of Pt for Cu sites can reduce the κ_{ph} down to 0.93 W m^{-1} K^{-1} at 300 K, which is comparable with that of ternary Al-Pd-Mn QC with heavier mean atomic weight.

Author Contributions: Conceptualization, Y.T.; methodology, S.O.; investigation, Y.T. and R.M.; writing—original draft preparation, Y.T. and R.M.; writing—review and editing, Y.T.; visualization, Y.T. and R.M.; supervision, A.-P.T.; funding acquisition, Y.T. All authors have read and agreed to the published version of the manuscript.

Funding: This work was partially supported by KAKENHI (Grant No. 17H03421, 19H05821, 20H02469) from the Japan Society for the Promotion of Science (JSPS).

Institutional Review Board Statement: Not applicable.

Informed Consent Statement: Not applicable.

Data Availability Statement: The data presented in this study are available on a reasonable request from the corresponding author.

Acknowledgments: One of the authors (Y.T.) acknowledges Kaoru Kimura, the University of Tokyo, for kind support on XRD and thermal conductivity measurements.

Conflicts of Interest: The authors declare no conflict of interest.

References

1. Snyder, G.J.; Toberer, E.S. Complex Thermoelectric Materials. *Nat. Mater.* **2008**, *7*, 105–114. [CrossRef]
2. Ren, Z.; Chen, G.; Dresselhaus, M. Nanostructured thermoelectric materials. In *Thermoelectrics and Its Energy Harvesting: Modules, Systems, and Applications in Thermoelectrics*; Rowe, D.M., Ed.; CRC Press: Boca Raton, FL, USA, 2012; Chapter 1.

3. Takagiwa, Y.; Kimura, K. Metallic-covalent bonding conversion and thermoelectric properties of Al-based icosahedral quasicrystals and approximants. *Sci. Technol. Adv. Mater.* **2014**, *15*, 044802. [CrossRef]
4. Takagiwa, Y.; Kamimura, T.; Hosoi, S.; Okada, J.T.; Kimura, K. Thermoelectric properties of polygrained icosahedral $Al_{71-x}Ga_xPd_{20}Mn_9$ (x = 0, 2, 3, 4) quasicrystals. *J. Appl. Phys.* **2008**, *104*, 073721. [CrossRef]
5. Takagiwa, Y.; Kamimura, T.; Okada, J.T.; Kimura, K. Thermoelectric Properties of Icosahedral Al-Pd-(Mn or Re) Quasicrystals: Improvement of the ZT Value by Ga Substitution for Al Atoms. *J. Electron. Mater.* **2010**, *39*, 1885–1889. [CrossRef]
6. Pierce, F.S.; Bancel, P.A.; Biggs, B.D.; Guo, Q.; Poon, S.J. Composition dependence of the electronic properties of Al-Cu-Fe and Al-Cu-Ru-Si semimetallic quasicrystals. *Phys. Rev. B* **1993**, *47*, 5670–5676. [CrossRef] [PubMed]
7. Bilušić, A.; Smontara, A.; Lasjaunias, J.C.; Ivkov, J.; Calvayrac, Y. Thermal and thermoelectric properties of icosahedral $Al_{62}Cu_{25.5}Fe_{12.5}$ quasicrystal. *Mater. Sci. Eng. A* **2020**, *294–296*, 711–714. [CrossRef]
8. Bilušić, A.; Pavuna, D.; Smontara, A. Figure of merit of quasicrystals: The case of Al-Cu-Fe. *Vacuum* **2001**, *61*, 345–348. [CrossRef]
9. Nakayama, R.; Takeuchi, T. Thermal Rectification in Bulk Material Through Unusual Behavior of Electron Thermal Conductivity of Al-Cu-Fe Icosahedral Quasicrystal. *J. Electron. Mater.* **2015**, *44*, 356–361. [CrossRef]
10. Dolinšek, J.; Vrtnik, S.; Klanjšek, M.; Jagličić, Z.; Smontara, A.; Smiljanić, I.; Bilušić, A.; Yokoyama, Y.; Inoue, A.; Landauro, C.V. Intrinsic electrical, magnetic, and thermal properties of single-crystalline $Al_{64}Cu_{23}Fe_{13}$ icosahedral quasicrystal: Experiment and modeling. *Phys. Rev. B* **2007**, *76*, 054201. [CrossRef]
11. Hurd, A.J.; Kelley, R.L.; Eggert, R.G.; Lee, M.-H. Energy-critical elements for sustainable development. *MRS Bull.* **2012**, *37*, 405–410. [CrossRef]
12. Takeuchi, T. Very large thermal rectification in bulk composites consisting partly of icosahedral quasicrystals. *Sci. Technol. Adv. Mater.* **2014**, *15*, 064801. [CrossRef] [PubMed]
13. Nagata, T.; Kirihara, K.; Kimura, K. Effect of Ru substitution for Re on the thermoelectric properties of AlPdRe icosahedral quasicrystals. *J. Appl. Phys.* **2003**, *94*, 6560–6565. [CrossRef]
14. Okada, J.T.; Hamamatsu, T.; Hosoi, S.; Nagata, T.; Kimura, K. Improvement of thermoelectric properties of icosahedral AlPdRe quasicrystals by Fe substitution for Re. *J. Appl. Phys.* **2007**, *101*, 103702. [CrossRef]
15. Edagawa, K.; Kajiyama, K.; Tamura, R.; Takeuchi, S. High-temperature specific heat of quasicrystals and a crystal approximant. *Mater. Sci. Eng. A* **2001**, *312*, 293–298. [CrossRef]
16. Prekul, A.F.; Kazantsev, V.A.; Shchegolikhina, N.I.; Gulyaeva, R.I.; Edagawa, K. High-Temperature Heat Capacity of the $Al_{63}Cu_{25}Fe_{12}$ Quasicrystal. *Phys. Solid State* **2008**, *50*, 2013–2015. [CrossRef]
17. Tamura, S.; Fukushima, K.; Tokumoto, Y.; Takagiwa, Y.; Edagawa, K. High-Temperature Specific Heat of Al-Cu-Ru Icosahedral Quasicrystals and 1/1 Crystal Approximants. *Mater. Trans.* **2021**, *62*, 356–359. [CrossRef]
18. Fukushima, K.; Suyama, H.; Tokumoto, Y.; Kamimura, Y.; Takagiwa, Y.; Edagawa, K. Comparative study of high-temperature specific heat for Al-Pd-Mn icosahedral quasicrystals and crystal approximants. *J. Phys. Commun.* **2021**, *5*, 085002. [CrossRef]
19. Takeuchi, T. Unusual Increase of Electron Thermal Conductivity Caused by a Pseudogap at the Fermi Level. *J. Electron. Mater.* **2009**, *38*, 1354–1359. [CrossRef]
20. Kirihara, K.; Kimura, K. Composition dependence of thermoelectric properties of AlPdRe icosahedral quasicrystals. *J. Appl. Phys.* **2002**, *92*, 979–985. [CrossRef]
21. Kim, H.-S.; Gibbs, Z.M.; Tang, Y.; Wang, H.; Snyder, G.J. Characterization of Lorenz number with Seebeck coefficient measurement. *APL Mater.* **2015**, *3*, 041506. [CrossRef]
22. Mizutani, U.; Sato, H.; Inukai, M.; Zijlstra, E.S. e/a determination for 4d- and 5d-transition metal elements and their intermetallic compounds with Mg, Al, Zn, Cd and In. *Philos. Mag.* **2013**, *93*, 3353–3390. [CrossRef]
23. Maciá, E.; Rodríguez-Oliveros, R. Theoretical assessment on the validity of the Wiedemann–Franz law for icosahedral quasicrystals. *Phys. Rev. B* **2007**, *75*, 104210. [CrossRef]
24. Cahill, D.G.; Pohl, R.O. Heat flow and lattice vibrations in glasses. *Solid State Commun.* **1989**, *70*, 927–930. [CrossRef]
25. Cahill, D.G.; Watson, S.K.; Pohl, R.O. Lower limit to the thermal conductivity of disordered crystals. *Phys. Rev. B* **1992**, *46*, 6131–6140. [CrossRef] [PubMed]
26. Kanatzidis, M.G. Nanostructured Thermoelectrics: The New Paradigm? *Chem. Mater.* **2010**, *22*, 648–659. [CrossRef]
27. Takagiwa, Y.; Kimura, K.; Sawama, K.; Hiroto, T.; Nishio, K.; Tamura, R. Thermoelectric properties of Tsai-type Au-Al-RE (RE: Yb, Tm, Gd) quasicrystals and approximants. *J. Alloys Compd.* **2015**, *652*, 139–144. [CrossRef]
28. Ishikawa, A.; Takagiwa, Y.; Kimura, K.; Tamura, R. Probing the pseudogap via thermoelectric properties in the Au-Al-Gd quasicrystal approximant. *Phys. Rev. B* **2017**, *95*, 104201. [CrossRef]